(79) NAGTEGAAL, J. C., PARKS, D. M., and RICE, J. R. (1974) On numerically accurate finite element solutions in the fully plastic range, *Comp. Meth. in Appl. Mech. and Engng*, **4**, 153–177.
(80) NAVARRO, A. and de los RIOS, E. R. (1987) A model for short fatigue crack propagation with an interpretation of the short-long crack transition, *Fatigue Fracture Engng Mater. Structures*, **10**, 169–186.
(81) NAVARRO, A. and de los RIOS, E. R. (1988) Short and long fatigue crack growth. A unified model, *Phil. Mag.*, **57**, 15–36.
(82) NAVARRO, A. and de los RIOS, E. R. (1988) A microstructural short fatigue crack equation. *Fatigue Fracture Engng Mater. Structures*, **11**, 383–396.
(83) NEALE, B. K., CURRY, D. A., GREEN, G., HAIGH, J. R., and AKHURST, K. N. (1985) A procedure for the determination of the fracture resistance of ductile steels, *Int. J. Pressure Vessels Piping*, **20**, 155–179.
(84) OROWAN, E. (1949) Fracture and strength of solids, *Reports on Progress in Physics*, **12**, 186–232.
(85) PARKS, D. M. (1991) Three dimensional aspects of HRR dominance. This volume, pp. 205–232.
(86) RICE, J. R. (1968) A path independent integral and the approximate analysis of strain concentration by notches and cracks, *J. Appl. Mech.*, **35**, 379.
(87) RICE, J. R. (1974) Limitations to the small scale yielding approximation for crack tip plasticity, *J. Mech. Phys. Solids*, **22**, 17–26.
(88) RICE, J. R. and TRACEY, D. M. (1969) On the ductile enlargement of voids in triaxial stress fields, *J. Mech. Phys. Solids*, **17**, 201–217.
(89) SCHWALBE, K.-H. and HELLMANN, D. (1984) Correlation of stable crack growth with the J-integral and the crack opening displacement, effects of geometry, size and material, GKSS Report 84/E/37, GKSS-Forschungszentrum Gesesthacht GmbH.
(90) SCHWALBE, K.-H. and GRUTER, L. (1991) Application of the engineering treatment model (ETM) to the prediction of the behaviour of a circumferential pipe. This volume, pp. 1125–1133.
(91) STEVENS, R. N. and GUIU, F. (1987) *EGF Newsletter*, No. 7, pp. 10–11.
(92) VITVITSKII, P. M., PANASYUK, V. V., and YAREMA, S. Ya. (1975) Plastic deformation around crack and fracture criterion, *Engng Fracture Mech.*, **7**, 305–319.
(93) WELLS, A. A. (1961) Unstable crack propagation in metals: cleavage and fast fracture, *Proc. Crack Propagation Symposium*, Cranfield Institute of Technology, Bedfordshire, vol. 1, p. 201.

W. Brocks and H. Yuan†*

Numerical Studies on Stable Crack Growth

REFERENCE Brocks, W. and Yuan, H., **Numerical studies on stable crack growth**, *Defect Assessment in Components – Fundamentals and Applications*, ESIS/EGF9 (Edited by J. G. Blauel and K.-H. Schwalbe) 1991, Mechanical Engineering Publications, London, pp. 19–33.

ABSTRACT In this paper ductile crack growth is studied numerically for five geometrically different specimens from the same material. Numerical results agree quite well with experimental records and it is verified that the J-integral is more sensitive to specimen geometries than CTOD δ_5 and CTOA values. Through analyses of plastic regions at the crack tip it is not verified that there exists a steady state field at the tip where stresses and strains are stationary and controlled by the J-integral. The relationships between J, δ_5, and CTOA are discussed.

Introduction

For several years stable crack growth in ductile materials has been studied experimentally, theoretically, and numerically. One of the intensive focuses of research is whether or not and for how long the existing crack parameters which were introduced originally for crack initiation, e.g., J-integral of Rice **(1)**, CTOD or δ_5 **(3)**, are able to control the ductile crack growth.

Some numerical studies **(2)(4)** have shown that a zone exists near to a crack tip in ductile materials where the J-integral represents the amplitude of the field singularity like the stress intensity factor does in elastic crack problems. At the same time the crack tip opening displacement (CTOD) is linear proportional to the J-integral **(2)** and therefore can describe the crack field too. However, as soon as the crack initiates, J loses its theoretical basis as fracture parameter and its numerical path-independency **(5)**. Hutchinson and Paris argued if the J-resistance curve increases quickly during crack extension and the crack extension is restricted within a small amount, then the J is able to control the crack growth. The experiments of Schwalbe and Hellmann **(3)** have shown that the modified CTOD parameter, δ_5, is able to correlate the crack possibly to larger crack extension than the J-integral does. Experiments **(15)** have proven qualitatively that the crack tip opening angle (CTOA) becomes constant after a small amount of crack extension. However, the 'small amount' still has not been defined quantitatively and its sensitivity to numerical calculations and insensitivity to changes of loads need to be further discussed.

In the present paper we will study critically some existing crack parameters during the large ductile crack growth with the finite element method **(7)**, to

* Bundesanstalt für Materialforschung und -prüfung, Berlin, FRG.
† Institut für Mechanik, Technische Universität Berlin, FRG; presently at GKSS-Forschungszentrum Geesthacht, 2054 Geesthacht, FRG.

re-examine the ability of some parameters to control ductile crack growth and to answer some of the questions mentioned above.

Finite element computations and analysed problems

In this paper, five specimens from aluminum alloy (see Table 1) were investigated by the finite element method **(7)**, namely two compact tension specimens (CT), two centre-cracked specimens (CCT), and one single edge cracked bending specimen (SECB), to study the effects of specimen geometries on the fracture parameter during crack growth. The material properties are: elastic modulus $E = 71\,600$ MN/m^2, yield stress $\sigma_0 = 317$ MN/m^2, and ultimate tensile stress $\sigma_U = 440$ MN/m^2. The referenced experimental data for these specimens (loading curves, δ_5 curves, and J-resistance curves) have been obtained by Schwalbe and Hellmann **(3)**.

The experiments were simulated by following the load line displacement records and all calculations were based on two dimensional models (plane stress or/and plane strain) and Prandtl–Reuss flow theory. The crack growth was modeled by using the node release technique without node shifting. The nodal forces were slowly released at each node in a simultaneous, nonlinear way to model an increment of crack growth. No singularities in the crack tip element were included since it is essentially impossible to implement the singular element at the crack tip when using the node release procedure to simulate crack extensions. The FE program and FE meshes used here were validated through a number of numerical computations and comparisons with ADINA calculations, see **(5)(8)**. A typical finite element mesh used in the crack tip field is shown in Fig. 1. All computations take the same mesh in the crack tip field. The meshes far from the crack tip for specimens 2, 3, and 5 are shown in Fig. 2(a)–(c).

To study the specimen geometry effects and to overcome the influences from its path-dependency, the J-integral was evaluated in the far field, where J is numerically path-independent also during large crack growth. The further studies about J distributions in the near-field and theoretical analyses of its behaviour in the crack tip field will be published elsewhere **(9)**.

For ductile crack growth there are two possible definitions of the crack tip opening displacement (CTOD), see Fig. 3. While after a little crack growth the displacement at the momentary crack tip $\delta_t(a)$ becomes constant, the displacement at the initial crack tip $\delta(a_0)$ increases monotonically with the crack length. Suppose the material is homogeneous, then, in contrast to crack initiations, the new crack profile must be straight; there may not exist any remaining plastic deformation on the new crack surface. This means that $\delta_t(a)$ can contain elastic deformation only and must be much smaller than CTOD for crack initiation. Figure 3 shows the relation between $\delta(a_0)$ and $\delta(a)$, supposing that the new crack face is straight and the crack tip opening angle (CTOA) remains constant during crack growing. Since CTOA is very small, then

$$\text{CTOA} \approx 2 \tan (\text{CTOA}/2) = \frac{\delta(a)}{\rho} = \frac{\delta(a_0) - \delta_{i0}}{\Delta a + \rho} \tag{1}$$

where δ_{i0} represents the remaining plastic displacement at the initial crack tip after crack initiation and is constant during ductile crack growth. From equation (1) follows

$$\delta(a_0) = \Delta a \ \text{CTOA} + \delta(a) + \delta_{i0} \tag{2}$$

The crack tip opening displacement $\delta(a_0)$ depends linearly on increment of crack growth, since CTOA and $\delta(a)$ are invariable under the condition of stable crack growth, thus the CTOD must be monotonically increasing with crack extensions.

If the effects of the displacement differences between the initial crack tip and the measuring point of δ_5 are to be neglected after some crack growth, we have

$$\delta_5 = \Delta a \ \text{CTOA} + \delta(a) + \delta_{5i} \tag{3}$$

where δ_{5i} is the remaining plastic displacement at the δ_5 measuring point after the initiation. Just like CTOD, δ_5 is a linear function of crack increment during stable crack growth.

Since in our numerical computations only rectangular isoparametric elements are used in the crack field the displacement near to the crack tip may

Table 1 Geometries of investigated specimens

Specimen No.	*Specimen*	*W (mm)*	*B (mm)*	a_0 *(mm)*	Δa_{Exp} *(mm)*	*Finite element model*
1	CT	50	5	25.1	14.44	pl. stress
2	CT	100	20	71	17.15	pl. stress & pl. strain
3	CCT	50	5	25.3	8.58	pl. stress
4	CCT	100	20	74	8.18	pl. stress & pl. strain
5	SECB	50	5	25.5	11.9	pl. stress

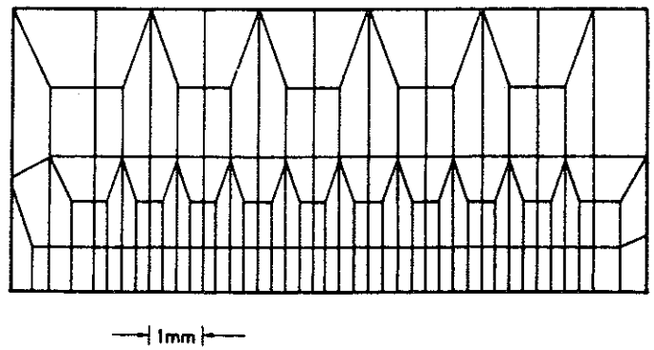

Fig 1 Details of mesh refinement in the vicinity of the growing crack

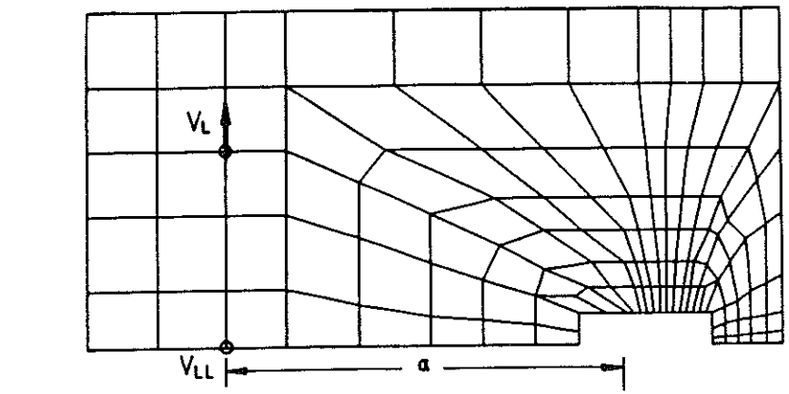

(a) Specimen 2 (CT)

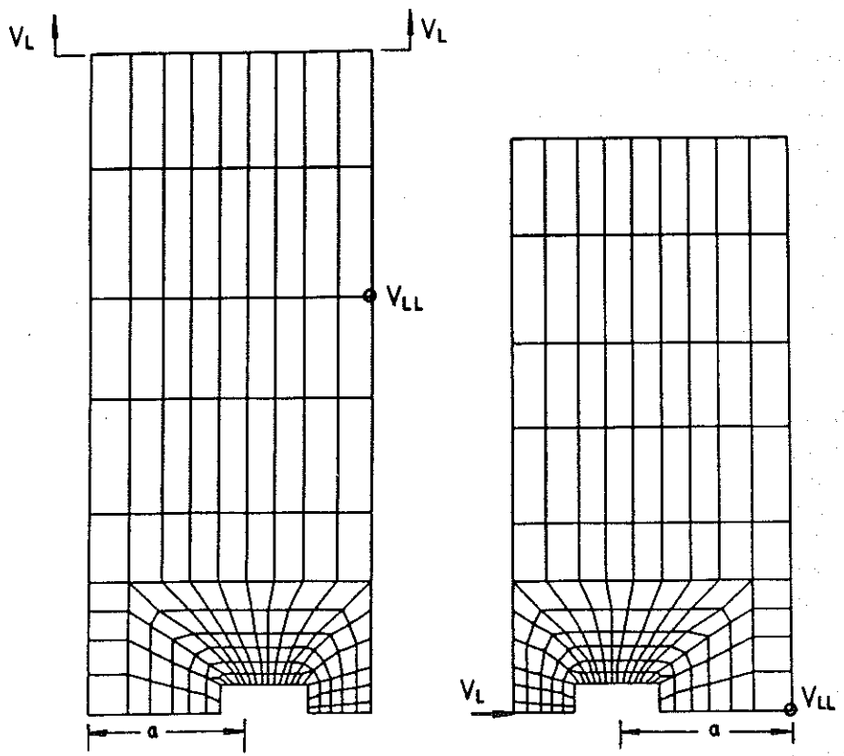

(b) Specimen 3 (CCT) (c) Specimen 5 (SECB)

Fig 2 Meshes in the far field

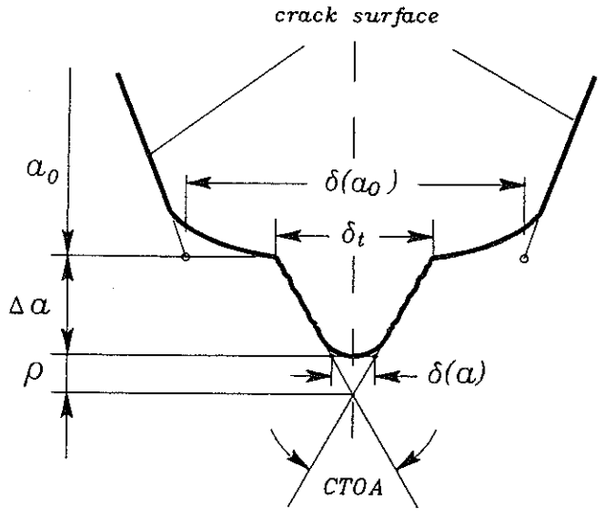

Fig 3 Sketch of crack tip profile

strongly depend on the size of the tip elements. Therefore, in this paper only the parameter δ_5 from Schwalbe *et al.* **(3)** instead of CTOD will be studied.

Numerical results and discussions

Figure 4 shows J-resistance curves from both experiments and numerical simulations of specimens Nos 1, 3, and 5. The J values are evaluated, just like the experiments, following the experimental formulas **(10)(11)**, to overcome the influence from calculating methods. All curves agree quite well with experimental records, although for large crack extensions little deviations in loading curves exist. The numerical J values at crack initiations for specimens Nos 1, 2, 4, and 5 are 17–28 N/mm and the correspondent experimental results are 22–23 N/mm. They overlap rather well and are independent on specimen geometry. A relatively large deviation from experimental records occurs for specimen No. 3 due to its high sensitivity to the crack initiation load. The comparison of plane stress and plane strain calculations, see Fig. 5, shows that even for both relatively thick specimens Nos 2 and 4 plane stress models crack growth clearly better than plane strain does. Whereas for small crack extension the two cases deviate a great deal from one another, with crack growth the deviation will be smaller.

While the plastic zone in plane strain calculations has a known butterfly shape in Mode I crack problem, the result from the plane stress calculation is shown in Fig. 6a. The shaded area in the figure denotes the plastic zone which is transformed from Gaussian integration points. The coordinates in Fig. 6 are normalized by the correspondent J-integral in the far field. After crack initiation the tip field is unloaded, and Figs 6(b) and (c) show changes of the plastic

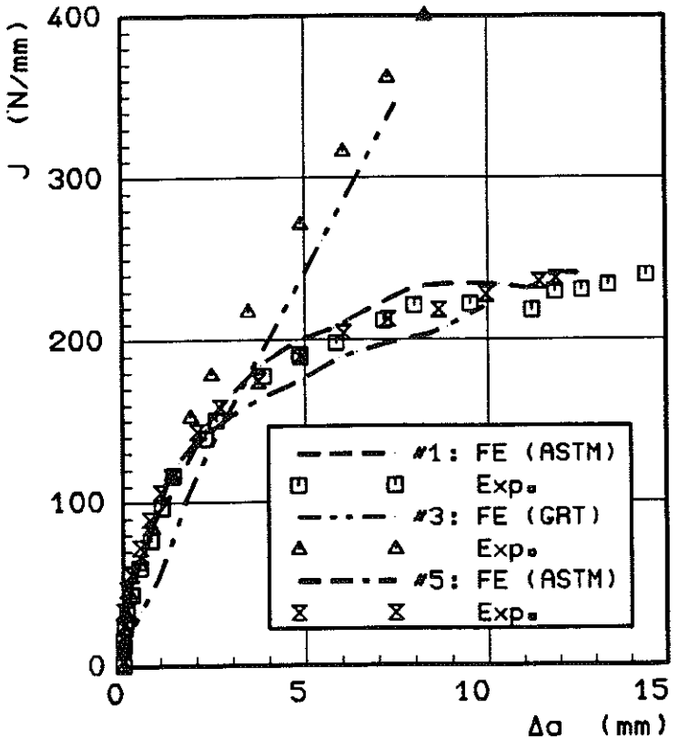

Fig 4 J_R **curves from experiment and FE calculation**

zone at the crack tip. The arrow in the figures denotes the present location of the crack tip.

Comparing Figs 6(b) and (c) the relative plastic zone in large crack growth is clearly smaller than in small crack growth. That is, the stress and the strain in the plastic region near to the crack tip are not proportional to the J integral which is evaluated in the far field. Although from the stress distributions there is a nearly steady state field at the momentary crack tip, no field exists which will be controlled by the J integral.

Under the known assumptions of invariable steady state crack tip field which consists of plastic and elastic angle sectors, see Fig. 7, Castañeda **(13)** has solved the crack tip field asymptotically in linear hardening elastic–plastic materials with the rate of tangent modulus α. It was shown that for $0.1 < \alpha < 1.0$ in the plane stress case the unloading angle lies between 73.65 and 79.92 degrees measured from the uncracked ligament ahead of the momentary crack tip. The asymptotic solutions extend the concept of a plastic reloading zone in elastic–perfectly plastic materials **(14)** to linear hardening materials and predict that in the plane strain cases of a material with the

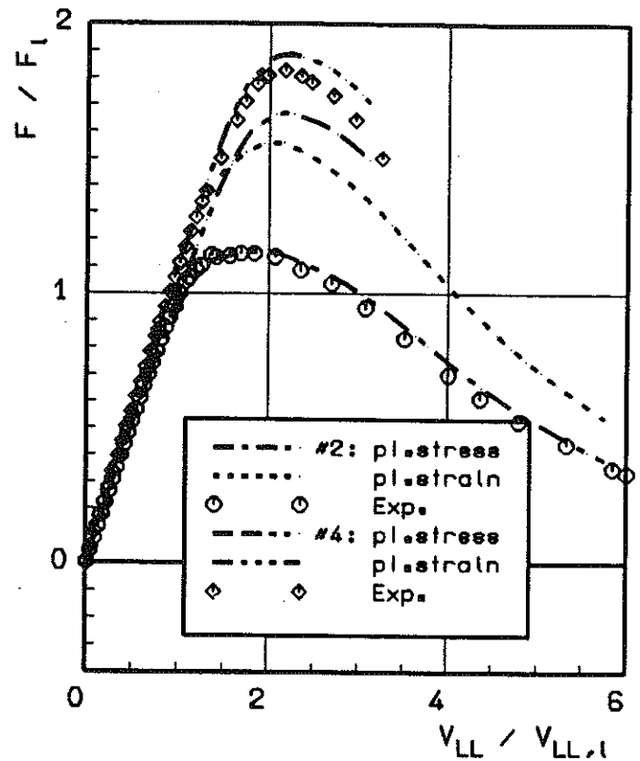

Fig 5 Comparison of plane strain and plane stress models

hardening factor $\alpha < 0.1$ the reloading plastic sector lies in $173.61 \leqslant \theta < 180$ degrees of the polar-coordinates centered at the crack tip. Contrary to the plane strain cases, the plane stress model can only contain the reloading angle nearly 180 degrees on the crack surfaces for all linear hardening materials.

Similar to analyses of the elastic–perfectly plastic FE computations in **(12)**, our numerical studies display that the unloading zone does not begin direct from the momentary crack tip, i.e., in the view point of numerical calculations there exists no plastic and elastic angle sectors around the crack tip, just like the active plastic zone and unloading wake zone, see Fig. 6.

All plane stress computations show, although there exists no clear unloading angle in the tip field, that any possible angle is larger than 90 degrees and does not agree with asymptotic prediction of **(13)**. The reason is possibly that numerical calculations have violated the assumption of small yielding region for asymptotic solution and the plastic zone is influenced by specimen boundaries.

Figure 6(d) shows that in the plane strain analyses there exists a plastic region behind the crack tip but nearly no reloading plasticity in the plane

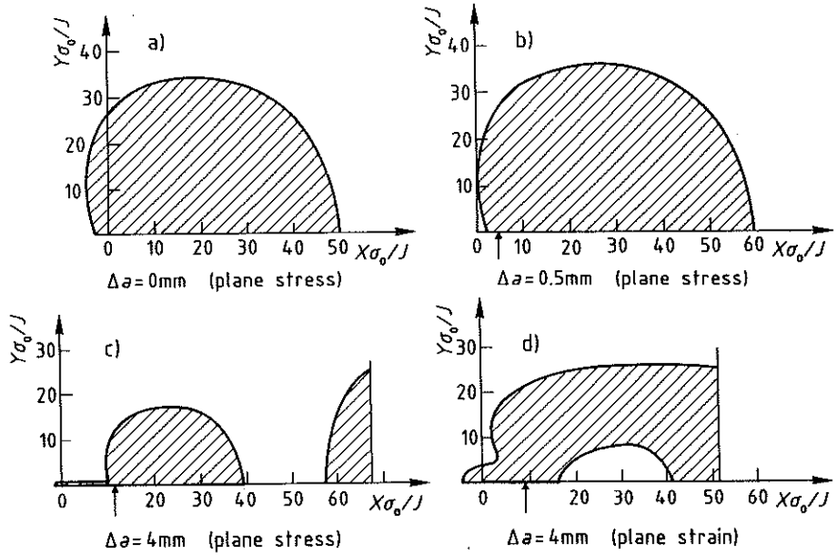

Fig 6 Plastic zones on the tip

stress computations, see Fig. 6(c), just like the prediction of asymptotic solution **(13)**. Some unregular plastic points in the plane stress analyses can only be accepted as numerical error from elastically unloading.

The distributions of stress component σ_{yy} in the first Gaussian points above the ligament ahead of the crack tip are shown in Fig. 8(a) for bending specimen No. 1 and in Fig. 8(b) for tension specimen No. 4 of the plane stress model. They differ little from each other in the near field though in the far field they are not comparable at all due to different loading configurations. Both figures show that after some crack extension the stress remains invariant or little changed, i.e., stresses become numerically independent of crack extensions. Under this condition the asymptotic solutions **(13)(14)** predict that

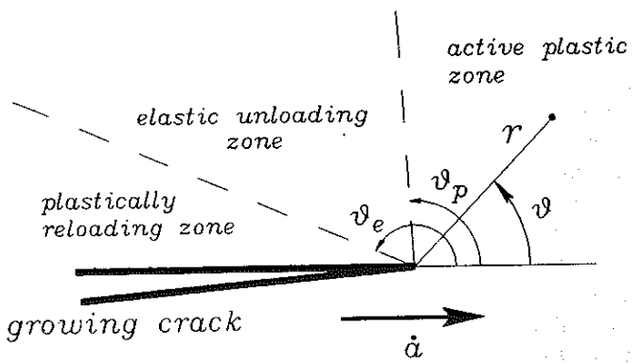

Fig 7 Angle sectors at crack tip in asymptotic analysis

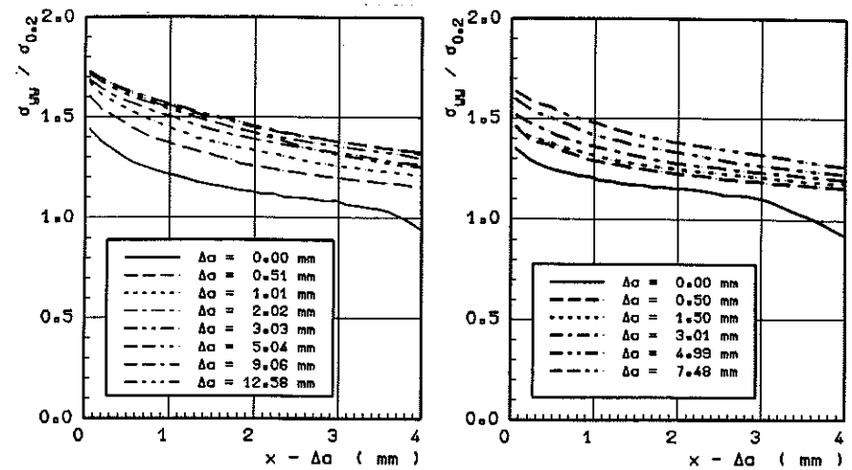

(a) spec. 1 (b) spec. 4

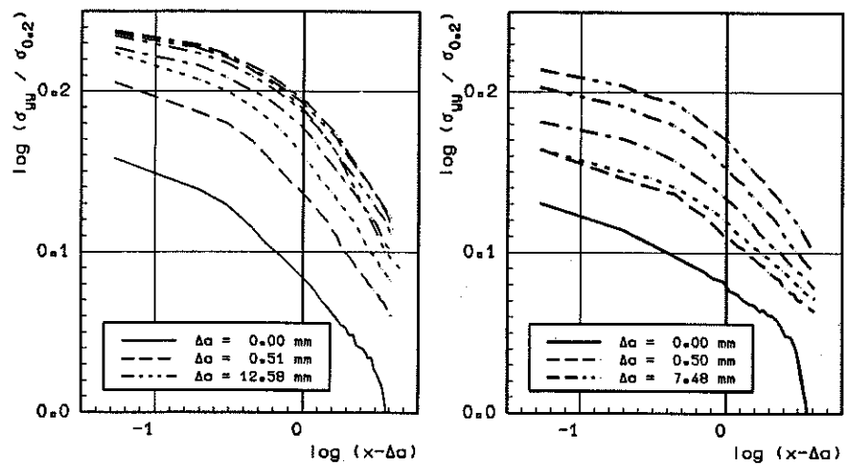

(c) spec. 1, logarithmic (d) spec. 4, logarithmic

Fig 8 Stresses σ_{yy} in the ligament ahead of the crack tip

stress and strain singularities must be much weaker than those in HRR-theory. This prediction is verified in some of our numerical studies. Figure 8(c) of specimen No. 1 shows the change of the singularities; the singularity decreases gradually from 0.037 at crack initiation to 0.020 at large crack propagation.

However, a similar result is not exhibited in Fig. 8(d) of specimen No. 4. Contrary to specimen No. 1, the singularity of stresses in specimen No. 4 is hardly changed at all. A definitive verification requires much finer finite element meshes and more numerical computations.

As many publications show, J resistance curves evaluated in the far field are dependent on specimen geometry, see Fig. 9. Also, even when the conditions from Hutchinson and Paris **(6)** are satisfied, the deviation of the curves is not negligible, see Table 2. Δa_J denotes the permitted maximal crack extension under the conditions in **(6)** and s_J stands for the deviation from the mean value

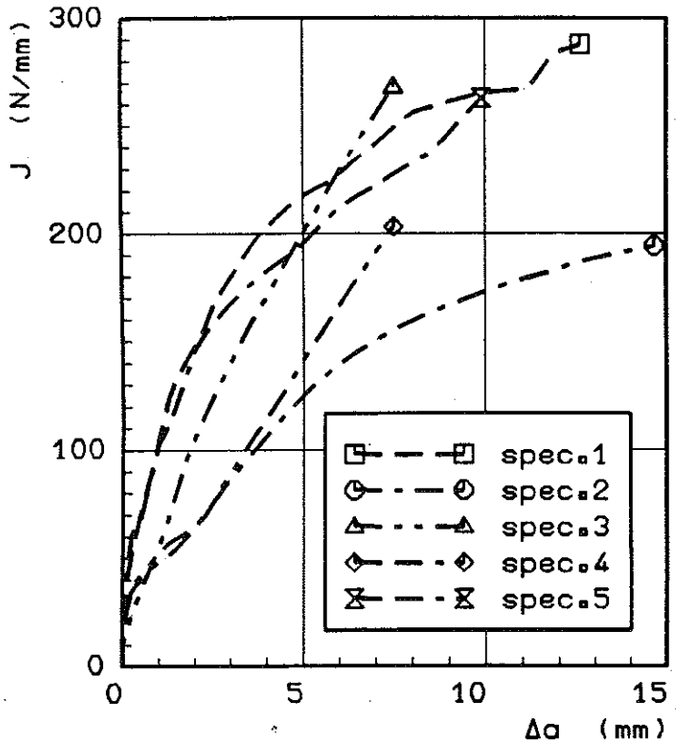

Fig 9 Geometry effects on J_R curves

Table 2

Specimen	*No. 1*	*No. 2*	*No. 3*	*No. 4*	*No. 5*
Δa_J (mm)	1.49	1.74	1.48	1.56	1.47
s_J (%)	41	−40	−13	−37	30
$s_{\delta 5}$ (%)	35	−30	12	−22	25
ϕ	0.127	0.094	0.10	0.10	0.114
γ (mm)	0.150	0.043	0.20	0.04	0.149
κ (mm^{-1})	−0.618	−0.485	—	—	−0.652
ζ	1.36	1.03	0.883	0.851	1.35

of the scatter band. The J-values of two thick specimens lie clearly under the curves of three thin ones. The resistance curves are more sensitive to the thickness of the specimens than to their form.

Figure 10 shows development of the crack tip profile during ductile crack growth of specimen No. 5. It can be seen that the crack surfaces formed during crack extension in both bending and tension specimens are straight near the momentary crack tip and are parallel to one another. There exists no obvious blunting at the momentary crack tip in contrast to the crack initiation. This means that CTOA remains constant and CTOD is nearly a linear function of crack increment, see equation (2). Our numerical results verify that the mean values of CTOA which will be evaluated through equation (2) are rather independent of specimen geometry, see Table 2. This relation must be also asymptotically correct for δ_5 if the remaining plastic deformation at the initial crack tip can be neglected. Comparison of different specimens shows that the crack tip profiles are little affected by specimen geometry.

The δ_5 curves from the numerical simulations agree excellently with the experimental records, see Fig. 11(a). Values of δ_5 show less dependence on

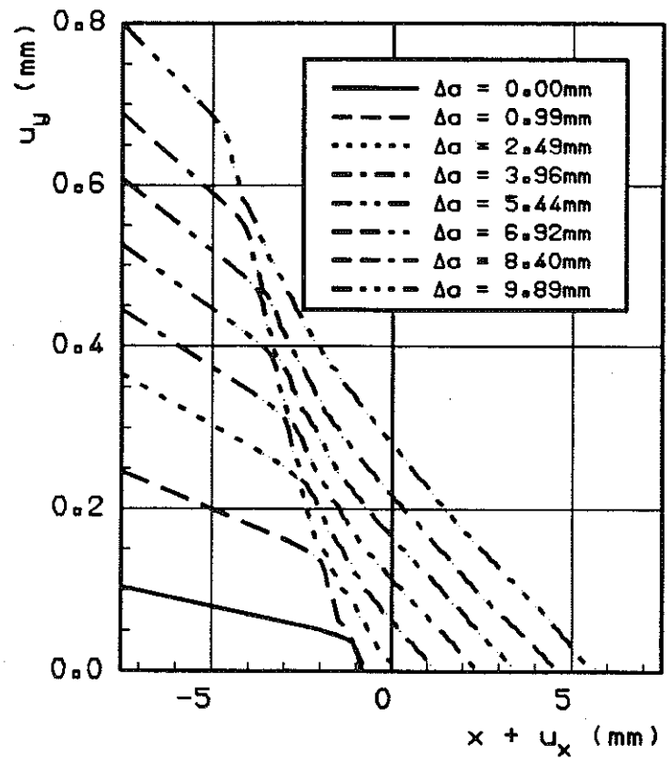

Fig 10 Crack opening profiles

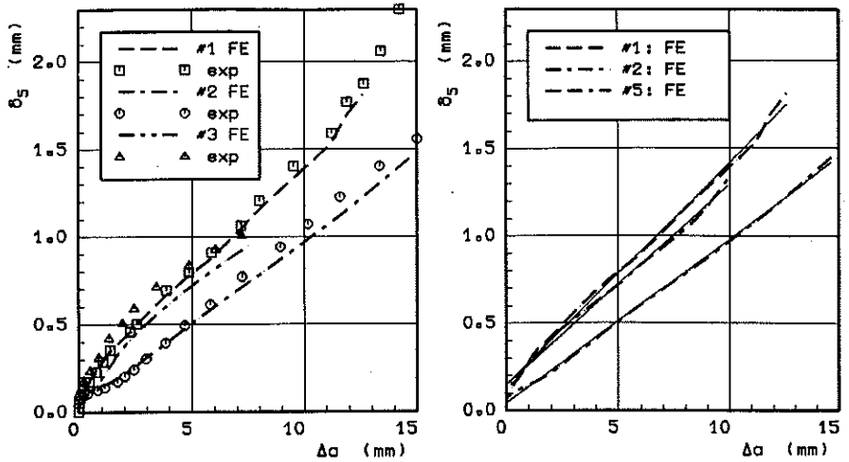

(a) comparison with experiment (b) linear curve fitting

Fig 11 δ_5 resistance curves

specimen geometry than the J-integral, and, in particular, they do not show so much dispersion with crack growth as the J_R curves. The scatter band of δ_5 resistance curves is clearly more narrow. The relative scatter at $\Delta a = \Delta a_j$ is summarized in Table 2 under $\mathfrak{s}_{\delta 5}$.

After a phase of crack extension the crack state remains invariant and it follows that the δ_5 resistance curves can be approximated through linear functions, see Fig. 11(b) and equation (3)

$$\delta_5 = \phi\ \Delta a + \gamma \tag{4}$$

where ϕ represents the average value of the crack tip opening angle in the whole crack extension process, and γ denotes the sum of CTOD at the momentary crack tip and the remaining plastic deformation in the crack tip region. These are listed in Table 2. Figure 11(b) shows that the linear function approximates the δ_5 resistance curves nearly exactly.

While for crack initiation there exists a linear relationship between J and CTOD, during stable crack growth this remains true for tension specimens only, see Fig. 12

$$\frac{J}{\sigma_{0.2}} = \zeta\ \delta_5 + \lambda \tag{5}$$

whereas in bend specimens the approximating function must be of a quadratic form

$$\frac{J}{\sigma_{0.2}} = \kappa\ \delta_5^2 + \zeta\ \delta_5 + \lambda \tag{6}$$

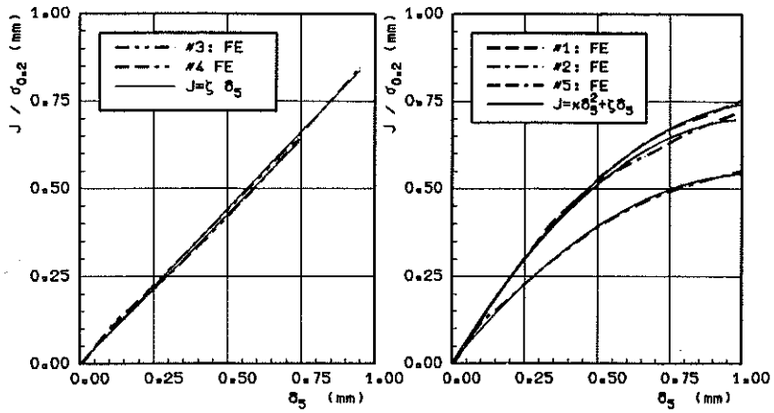

(a) tensile specimens (b) bend specimens

Fig 12 Relationship between J and CTOD

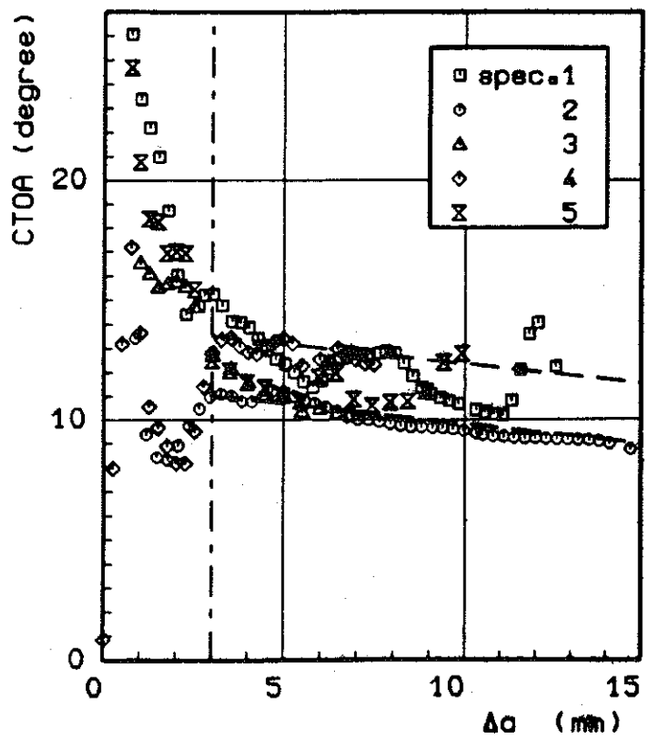

Fig 13 CTOA resistance curves

where factors κ, ζ, and λ are summarized in Table 2.

Although crack tip profiles in Fig. 10 appear quite similar to one another, the evaluation from the tip deformations is very sensitive in numerical calculation, see Fig. 13. Just as predicted from δ_5 curves, the CTOA curves, excluding the curve oscillations possibly due to numerical errors, are little influenced by specimen geometry for large crack extensions. Compared with the development of the plastic region at the crack tip, the CTOA comes to stable phase when the plastic zone extends through the uncracked ligament.

Conclusions

Ductile crack growth of CT, CCT, and SECB specimens have been analysed with the finite element method under both plane stress and plane strain conditions. The numerical results for all specimens agree well with the experimental data.

The analyses of plastic zones at the momentary crack tip show that the J-integral can no longer represent the stress state in the crack tip field during crack extension. In our numerical studies some evidence for the asymptotic analyses about changes of stress and strain singularities in linear hardening material is revealed. The existence of a plastically reloading zone which was predicted by asymptotic solutions in the plane strain case is verified in our numerical calculations, while the angular sectors and the angle of the unloading boundary do not agree with each other. A definitive prediction, however, needs much finer finite element mesh in the near field.

Numerical J- and δ_5-resistance curves depend on the specimen geometry, although all conditions from Hutchinson and Paris **(6)** are satisfied. δ_5 curves have a smaller scatter band than J-resistance curves. During crack extension the CTOA curves are little affected by specimen geometry when specimens become fully plastic.

During stable crack extension δ_5 depends linearly on crack increment, that is, under this condition, δ_5 is equivalent to the CTOA. A linear relationship between J and CTOD exists only for tension specimens, while for bending specimens it is a quadratic function.

Acknowledgements

This work was supported by the Deutsche Forschungsgemeinschaft (DFG) under contract number Br 521/2-1. The authors thank Dr D. Hellmann of GKSS-Forschungszentrum Geesthacht for the experimental data.

References

(1) RICE, J. R. (1968) A path-independent integral and the approximate analysis of strain concentration by notches and cracks, *J. Appl. Mech.*, **35**, 379–386.

(2) SHIH, C. F., DELORENZI, H. G., and ANDREWS, W. R. (1979) Studies on crack initiation and stable crack growth, *Elastic–Plastic Fracture, ASTM STP 668* (Edited by Landes J. D. *et al.*), pp. 65–120, ASTM, Philadelphia.

(3) SCHWALBE, K.-H. and HELLMANN, D. (1984) Correlation of stable crack growth with the J-integral and the crack tip opening displacement, effects of geometry, size, and material, *GKSS Report 84/E/37*, GKSS-Forschungszentrum Geesthacht GmbH.

(4) BROCKS, W. and OLSCHEWSKI, J. (1986) On J-dominance of crack-tip fields in largely yielded 3-D structures, *Int. J. Solids Structures*, **22**, 693–708.

(5) BROCKS, W. and YUAN, H. (1989) Numerical investigations on the significance of J for large stable crack growth, *Eng. Fracture Mechanics*, **32**, 459–468.

(6) HUTCHINSON, J. W. and PARIS, P. C. (1979) Stability analysis of J-controlled crack growth in *Elastic–Plastic Fracture, ASTM STP 668* (Edited by Landes J. D. *et al.*), pp. 37–63, ASTM, Philadelphia.

(7) BROCKS, W. and YUAN, H. (1990) Fe-Analysen des Rißwiderstandsverhalten dünner Proben bei großem Rißwachstum, *BAM Report 1.01 90/4*, Bundesanstalt für Materialforschung und -prüfung (BAM), Berlin.

(8) BARTMANN, S., BROCKS, W., and YUAN, H. (1989) Bruchmechanische Parameter zur Beschreibung von stabilem Rißwachstum in duktilem Material (in German), *Berichtsband 13. Sitzung des Arbeitskreises Bruchmechanik*, Deutscher Verband für Materialforschung und -prüfung (DVM), Berlin.

(9) YUAN, H. (1990) Untersuchung bruchmechanischer Parameter für elastisch–plastisches Rißwachstum, *Fortschr.-Ber. VDI Reihe 18, Nr. 82*, VDI-Verlag, Düsseldorf.

(10) Standard test for J_{Ic}, a measure of fracture and toughness, *E 813 – 81* (1980) *Annual Book of ASTM Standards*, Part 10, ASTM, Philadelphia.

(11) GARWOOD, S. J., ROBINSON, J. N., and TURNER, C. E. (1975) The measurement of crack growth resistance curves using the J-integral, *Int. J. Fracture*, **11**, 528–530.

(12) SHAM, T.-L. (1983) A finite element study of the asymptotic near-tip fields for mode I plane strain cracks growing stably in elastic–ideally plastic solids, *Elastic–Plastic Fracture: 2nd Symp., Vol. I, ASTM STP 803* (Edited by Shih C. F. and Gudas J. P.), pp. I52–I79, ASTM, Philadelphia.

(13) CASTAÑEDA, P. P. (1987) Asymptotic fields in steady crack growth with linear strain hardening, *J. Mech. Phys. Solids*, **54**, 227–268.

(14) DRUGAN, W. J., RICE, J. R., and SHAM, T.-L. (1982) Asymptotic analysis of growing plane strain tensile cracks in elastic–ideally plastic solids, *J. Mech. Phys. Solids*, **447**, 473.

(15) KANNINEN, M. F. and HAHN, G. T., *et al.* (1980) Development of a plastic fracture methodology, *Final Report to EPRI, NP-1734, Research Project 601-1*, Columbia Laborotories, Battelle.